Polymer brush bilayers at thermal equilibrium: A theoretical approach†

Majid Farzin

Starting from statistical mechanics of polymers and using density functional theory (DFT) method, I review theory of polymer brush bilayers at thermal equilibrium thorough a novel point of view. Density profiles, brush heights and interpenetration length in terms of molecular parameters and distance between substrates are obtained at thermal equilibrium. With a transparent analytic approach, it is being shown, how polymer brushes balance compression and elasticity when bilayers of brush come into contact. Pressure is calculated and it is shown that substrates might repel, attract or even do not see each other upon varying system parameters. Uniqueness of the results, based on taking deformations of both brushes into account, suggests that existing theories about polymer brush bilayers (blob picture) need highly likely to be reviewed.

1 Introduction

Polymers are a class of long macromolecules that consist of repeated units of atoms or molecules i.e. monomers[1]. Connectivity among monomers in a polymer chain is fulfilled through sharing valance electrons i.e. covalent or molecular bond. Monomers undergoing Brownian motions constantly change shape of whole polymer chain so that in long time polymer chain undergoes all possible conformations. Statistical mechanics in canonical ensemble is the most appropriate theoretical tool for equilibrium properties of a polymer chain[2].

Polymer brushes are a class of polymeric structures that are present in many practical situations[3]. They consist of densely grafted polymer chains to surfaces and they swell due to steric repulsion among monomers of nearby chains[3]. Polymer brushes have already been approached by many theoreticians[4–8]. Two opposing brush covered surfaces form a polymer brush bilayer[3]. Polymer brush bilayers are present in a wast majority of biological systems such as mammalian knee joints as lubricant[3]. Compressed polymer brush bilayers are known to interpenetrate which is source of lubrication and shear thinning effects. There have been already theoretical approaches to polymer brush bilayer problem which reader may be interested in them[9–15]. However, I believe theoretical works already published lack a transparent approach to the problem of polymer brush bilayers. For the sake of clarity as well as developing a strong theoretical framework for this problem, I review theory of polymer brush bilayers from the scratch through a novel theoretical point of view.

2 Polymer in external force

Conformation of a polymer chain changes due to Brownian motion of its monomers. Theoretically, this situation could be assumed as N vectors of length a that are connected together and are free to rotate in three dimensional space. To obtain elastic properties of chain, we need to apply a force field to chain and observe its behavior and at the end remove the force field from the resulting quantities. The remaining leading order terms represent elastic properties of chain in absence of force field.

First of all, I introduce Hamiltonian of the system as summation of inner products of force field with all vectors. Negative sign ensures that minimum energy takes place when all vectors purely align toward force field. So, conformations of polymer chain are determined by θ, the smaller angle between force field and vectors. For simplicity and symmetry considerations, I choose spherical polar coordinates and apply force field in z direction. So, the angle between force field and vectors is the same as polar angle θ in spherical polar coordinates.

$$H = -fa\sum_{i=1}^{N}\cos\theta_i \tag{1}$$

Having introduced the Hamiltonian, it will be the next step to calculate partition function which is defined as $Z = \int d\Omega \exp -H/k_{\mathrm{B}}T$ where Ω denotes all possible conformations of chain. The partition function turns out to following integral in spherical polar coordinates,

$$Z(f,T) = \left(2\pi a^2\int_0^{\pi} e^{\zeta\cos\theta}\sin\theta\, d\theta\right)^N \tag{2}$$

Where I introduce new variable $\zeta = af/k_{\mathrm{B}}T$. The above integral is simply solvable due to uncorrelated vectors (monomers) and it gives the following result for the partition function,

$$Z(f,T) = \left(4\pi a^2\frac{\sinh\zeta}{\zeta}\right)^N \tag{3}$$

Having obtained the partition function, we can simply calculate

[a] E-mail: farzin.ph@gmail.com

canonical free energy as $F(f,T) = -k_{\mathrm{B}}T\log Z(f,T)$ giving following expression,

$$F(f,T) = -Nk_{\mathrm{B}}T\log\left(4\pi a^2\frac{\sinh\zeta}{\zeta}\right) \tag{4}$$

This is the free energy at constant force and temperature. Since, I fixed the force and temperature, so the length of the polymer chain fluctuates. The mean value of the length can be obtained from the canonical free energy as $-\partial F(f,T)/\partial f$ which gives us the following length,

$$\langle L\rangle = Na\left(\coth\zeta - \frac{1}{\zeta}\right) \tag{5}$$

The expectation value of polymer chain length can alternatively be calculated from direct integration which is equal to above result. In statistical mechanics, $\coth\zeta - \zeta^{-1}$ is called the *Langevin* function[2]. As it is observed, the expectation value of polymer chain length subject to an external force is non-zero. Certainly, this occurs, exclusively, along external force (here z direction) and in other directions (here x and y directions) the average length vanishes. To obtain fluctuations of polymer chain we need to have mean square length i.e. $\langle L^2\rangle$. Mean square length can be calculated through integration to give following result,

$$\langle L^2\rangle = Na^2 \tag{6}$$

and fluctuation in polymer length via $\langle L^2\rangle - \langle L\rangle^2$ giving following result,

$$\Delta L^2 = Na^2 - N^2a^2\left(\coth\zeta - \frac{1}{\zeta}\right)^2 \tag{7}$$

The susceptibility $\partial^2F(f,T)/\partial f^2$ at fixed force and temperature reads as follows,

$$\kappa = \frac{Na^2}{k_{\mathrm{B}}T}\left(\mathrm{csch}^2\zeta - \frac{1}{\zeta^2}\right) \tag{8}$$

It is interesting to see the behavior of a polymer chain at fixed length and temperature that can be achieved by Helmholtz free energy $A(L,T) = F(f,T) + f\langle L\rangle$ as follows,

$$A(L,T) = Nk_{\mathrm{B}}T\left(\zeta\coth\zeta - \log\left(4\pi a^2\frac{\sinh\zeta}{\zeta}\right) - 1\right) \tag{9}$$

In this section, I reviewed the thermodynamics of a polymer chain via statistical mechanical point of view. I obtained exact solutions for thermodynamic quantities. They will get more reliable when we consider asymptotic behaviors of the results which I will do in the nest two sections.

3 Polymer in weak external force

In most situations, magnitude of the external force is much smaller than thermal energy. In this limiting case, I can consider the dimensionless quantity $\zeta \ll 1$ much smaller than unity and make Taylor expansion of the physical quantities. The Taylor expansions give us following terms,

$$F(f,T) = -Nk_{\mathrm{B}}T\log\left(4\pi a^2\right) - Nk_{\mathrm{B}}T\left(\frac{1}{6}\zeta^2 + O\left(\zeta^4\right)\right) \tag{10}$$

The first term in canonical free energy is the free energy of N freely rotating vectors of fixed length a in three dimensional space. The second term is the leading order term in terms of the external force. This term has most of the information about a polymer chain. Looking at Eqs. 11 and 12, we see that this term can be rewritten as $\frac{1}{2}\kappa^{-1}\langle L\rangle^2$. This is a free energy which introduces us elasticity due to entropy in a polymer chain. This term tries to shrink the chain. The inverse compressiblity or susceptibility plays role of spring constant but with a difference to crystals. The elastic constant in solids decreases by temperature but in a polymer and rubber-like materials the elastic constant increases by temperature. So, by heating up the polymers they contract due to $\langle L\rangle = f/\kappa^{-1}$ in contrast to crystalline materials.

$$\langle L\rangle = Na\left(\frac{1}{3}\zeta + O\left(\zeta^3\right)\right) \tag{11}$$

In Eqs. 11 and 12 average length and compressiblity of the chain is seen in weak external force. The leading order term in average length depends on external force so in absence of external force the average length vanishes as it is expected. Naturally, when a polymer chain is subject to an external force, it tends to align to the force direction. This causes non-zero average length which occures in absence of external force.

$$\kappa = \frac{a^2N}{3k_{\mathrm{B}}T}\left(1 - \frac{1}{5}\zeta^2 + O\left(\zeta^4\right)\right) \tag{12}$$

The leading order term of compressibility is independent of external force. It gives an intrinsic property of polymer chain $\kappa^{-1} = \frac{3k_{\mathrm{B}}T}{a^2N}$ which indicates the elasticity originated from entropy.

$$\Delta L^2 = a^2N - N^2a^2\left(\frac{1}{9}\zeta^2 + O\left(\zeta^4\right)\right) \tag{13}$$

The fluctuation of chain length in weak external force is extremely interesting quantity. To understand which term dominates in the perturbation expansion, we need to compare their magnitude. Since the second term is $\sim N^2$ it appears to dominate the first term but it is multiplied by the perturbation coefficient squared ζ^2. So to see which term dominates we need to make numerical comparison. Typical polymer chains consist $N = 10^5$ monomers and usually force is in order of pN and a monomer has size of 0.1 nm. Considering order of magnitude of the Boltzmann constant as 10^{-23} and room temperature $T = 300$K, the perturbation coefficient gets $\zeta \sim 10^{-2}$. Consequently, the first and the second terms have almost same order of magnitude and both are leading order terms. As it is expected when temperature increases the fluctuations of the chain length increases as well and in extreme limit of $T \to \infty$ then $\Delta L^2 \to a^2N$. It means than at very large temperatures, the length fluctuations equals the mean square length. Interestingly, in presence of external force, fluctuations are small compared to mean squared length but in absence of external force, fluctuations equal mean squared length. It means that under the influence of external force, the chain is

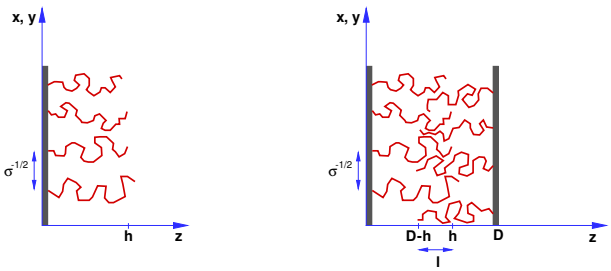

Fig. 1 Schematic view of a polymer brush (left) and a polymer brush bilayer (right).

elongated along the force direction and shows minor fluctuations in length.

$$A(L,T) = -Nk_{\mathrm{B}}T\log\left(4\pi a^2\right) + Nk_{\mathrm{B}}T\left(\frac{1}{6}\zeta^2 + O\left(\zeta^4\right)\right) \tag{14}$$

The Helmholtz free energy at fixed length and temperature shows that at small external forces, elasticity of a polymer chain is $\kappa^{-1}\langle L\rangle^2/2$. This is an important result that will be used in the next section as the free energy of a polymer chain.

4 Polymer in strong external force

Another interesting case is a very strong external force applied to a polymer chain. In this limit, the chain stretches extremely and at sufficiently large forces the chain becomes a line. The behavior of physical quantities under this extreme condition can be seen by making limit of them when external force approaches infinity.

$$\begin{aligned}
\lim_{f\to\infty} F(f,T) &\to -\infty \\
\lim_{f\to\infty} \langle L\rangle &\to Na \\
\lim_{f\to\infty} \langle L^2\rangle &\to Na^2 \\
\lim_{f\to\infty} \Delta L^2 &\to Na^2 - N^2a^2 \\
\lim_{f\to\infty} \kappa &\to 0 \\
\lim_{f\to\infty} A(L,T) &\to \infty
\end{aligned} \tag{15}$$

Interestingly, average length goes to Na as it is expected from rod limit. The squared length fluctuations goes to $Na^2 - N^2a^2$ as rod limit achieved but this this a negative value and it is an imaginary quantity. Therefore, I would say at rod limit length fluctuations has no real quantity. The susceptibility goes to zero i.e. the elasticity goes to infinity that means a very stiff spring resembling rod limit. Both free energies go to infinity at rod limit.

5 Polymer brushes

Polymer brushes are composed of linear polymer chains densely grafted to a surface[3]. The steric repulsion between monomers of nearby chains swells any chain to collectively form brush-like structure. Here, I review theoretical analysis of polymer brushes through density functional theory. I assume polymer chains grafted with density σ to a substrtate at $z = 0$ (See Fig. (1)). I start from grand potential functional as follows,

$$\Phi[n(z)] = \int_0^h \left(\frac{3k_{\mathrm{B}}Tz^2}{a^2N^2}n(z) + \frac{b}{2}k_{\mathrm{B}}Tn(z)^2 - \mu\, n(z)\right)dz \tag{16}$$

The first term in Eq. 16 refers to leading order term of Helmholtz free energy which describes elastic energy coming from entropy in chain. Since energy is distributed throughout the chain according to probability distribution function, I multiply Helmholtz free energy by $P(z) = n(z)/N$. The second term is quadratic in monomer concentration and it takes the excluded volume interactions among monomers. The quadratic term refers to the first correction to free energy of a gas based on consideration of binary interactions among monomers. Here, $b = (1/2)\int d^3r\,(1-\exp(-U(r)/k_{\mathrm{B}}T))$ is the second virial coefficient that represents strength of binary correlations among monomers. For hard spheres of diameter a, $b = (2\pi/3)a^3$ independent of temperature. For Lennard-Jones particles $b = (2\pi/3)a^3\left(\frac{1.73}{\bar{T}^{1/4}} - \frac{2.56}{\bar{T}^{3/4}} + \ldots\right)$ with $\bar{T} = k_{\mathrm{B}}T/\varepsilon^2$.

The equilibrium density profile, brush height and chemical potential are to be obtained through simultaneous solution of following coupled equations. The first equation sets a functional derivative of grand potential with respect to monomer density profile. It leads to an Euler-Lagrange differential equation. The solution of corresponding Euler-Lagrange differential equation gives the equilibrium density profile of polymer brush.

The second equation refers to derivative of grand potential with respect to brush height having inserted the equilibrium density profile in it. The third equation indicates that total number of monomers in polymer brush is obtained through integration over the equilibrium density profile throughout brush region.

$$\begin{aligned}
\frac{\delta\Phi[n(z)]}{(z)} &= 0 \\
\frac{\partial\Phi[n(z)]}{\partial h} &= 0 \\
\int_0^h n(z) &= N\sigma
\end{aligned} \tag{17}$$

Solving Eqs. 17, gives following results,

$$
\begin{aligned}
n(z) &= \frac{3\sigma^{2/3}}{2^{2/3}a^{2/3}b^{1/3}} - \frac{3z^2}{a^2N^2b} \\
h &= \frac{a^{2/3}b^{1/3}N\sigma^{1/3}}{2^{3/2}} \\
\mu &= 3k_{\mathrm{B}}T\left(\frac{b\sigma}{2a}\right)^{2/3}
\end{aligned} \tag{18}
$$

Eq. 18 shows a parabolic density profile for brush together with universal power laws of brush height and chemical potential in terms of molecular parameters. Here, brush height and chemical potential follow universal power laws in terms of molecular parameters.

Inserting Eq. (22) into Eq. (17) gives us the following grand potential energy in terms of molecular parameters,

$$
\Phi = -\frac{3}{5}Nk_{\mathrm{B}}T\left(\frac{2^{1/3}\,b^{2/3}\,\sigma^{5/3}}{a^{2/3}}\right) \tag{19}
$$

which indicates that the grand free energy is negative and scales with molecular parameters.

6 Polymer brush bilayer

Polymer brush bilayer is a system that has been observed in a wide range of physical systems from biology to industry. The most designated application for polymer brush bilayers is devoted to lubrication inside mammalian Synovial joints. To understand theoretically the equilibrium properties of a polymer brush bilayer system, I consider two polymer brush covered flat plates at $z=0$ and $z=D$ (See Fig. (1)).

I start from following grand potential where the first integral represents the bottom brush, the second integral represents the top brush and the third integral represents the steric repulsion among monomers of two brushes through interpenetration length. The two brushes are totally same in context of the molecular parameters so to take the second brush into account, it suffices to transform $z \longrightarrow (z-D)$ in entropic elasticity term plus integrating from top brush height $(D-h)$ to D. To take the excluded volume interactions among two brush layers we can integrate over multiplication of their densities profiles within their interpenetration region i.e. from $(D-h)$ to h.

$$
\begin{aligned}
\Phi[n(z),m(z)] &= \int_0^h \left(\frac{3k_{\mathrm{B}}Tz^2}{a^2N^2}\,n(z) + \frac{b}{2}\,k_{\mathrm{B}}T\,n(z)^2 - \mu\,n(z)\right)dz \\
&+ \int_{D-h}^{D}\left(\frac{3k_{\mathrm{B}}T(z-D)^2}{a^2N^2}\,m(z) + \frac{b}{2}\,k_{\mathrm{B}}T\,m(z)^2 - \mu\,m(z)\right)dz \\
&+ \frac{b}{2}\,k_{\mathrm{B}}T\int_{D-h}^{h} n(z)\,m(z)\,dz
\end{aligned} \tag{20}
$$

Having introduced the grand potential functional, solving the equations bellow lead to achieve equilibrium density profiles, height and chemical potentials corresponding to each brush layer. I note here that it suffices to take derivative of grand potential functional with respect to h as well as to calculate total monomers of bottom brush for calculations. This becomes possible due to similarity of two brushes.

$$
\begin{aligned}
\frac{\delta\Phi[n(z),m(z)]}{\delta n(z)} &= 0 \\
\frac{\delta\Phi[n(z),m(z)]}{\delta m(z)} &= 0 \\
\frac{\partial\Phi[n(z),m(z)]}{\partial h} &= 0 \\
\int_0^h n(z) &= N\sigma
\end{aligned} \tag{21}
$$

Eqs. 21 lead to following results for segment density profiles, brush heights and chemical potentials. Note that height of top brush is located at $(D-h)$.

$$
\begin{aligned}
n(z) &= \frac{\eta^2 + \frac{2D^3}{\eta} + 2D(\eta-4z) + \frac{D^4}{\eta^2} - D^2 - 4z^2}{2a^2bN^2} \\
m(z) &= \frac{\eta^2 + \frac{2D^3}{\eta} + 2D(\eta+8z) + \frac{D^4}{\eta^2} - 13D^2 - 4z^2}{2a^2bN^2} \\
h &= \frac{1}{2}\left(\eta + D\left(\frac{D}{\eta}-1\right)\right) \\
\mu &= k_{\mathrm{B}}T\,\frac{3\left(2D\eta + \eta^2 + \frac{2D^3}{\eta} + \frac{D^4}{\eta^2} - 5D^2\right)}{4a^2N^2}
\end{aligned} \tag{22}
$$

where η is a length scale which is defined as follows,

$$
\eta = \left(\sqrt{3a^2bN^3\sigma\left(3a^2bN^3\sigma - 2D^3\right)} + 3a^2bN^3\sigma - D^3\right)^{1/3}
$$

Having brush heights an important quantity here is interpenetration length between two brushes which is equal to $2h-D$ leading the following result,

$$
l = \frac{(D-\eta)^2}{\eta} \tag{23}
$$

In Fig. 2, I present density profiles of polymer brush layers, their overlap density profile and density profile of an isolated brush Eq. (16) to see visually how it changes under contact to top brush. I choose $a=1$, $b=2.09$, $\sigma=0.1$, $N=30$ and $D=15$. It is seen that brushes compressed due to contact with each other. This is an important point since we see a balance between elasticity of brushes and compressive force from other brush side. Density profiles of polymer brush layers possesses three major properties; larger density of monomers in vicinity of surfaces, smaller thickness and non-parabolic (almost linear) functionality in terms of perpendicular direction (z direction).

In Fig. 3, I present interpenetration length in terms of wall distance. This plot, in contrast to what has been claimed in works already published, does not fit to any universal power law. However, interpenetration length decreases as wall distance increases

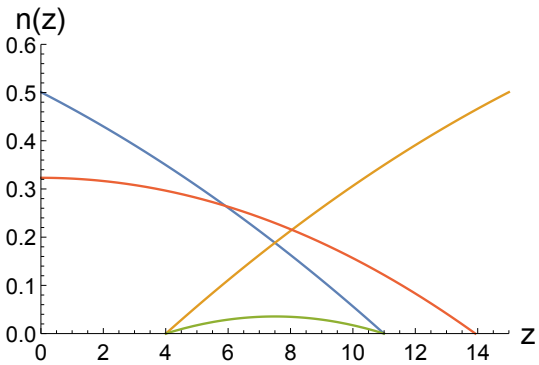

Fig. 2 Density profiles of bottom brush (blue), top brush (orange), the overlap density profile of bottom and top brushes (green) and density profile of bottom brush in absence of top brush (red).

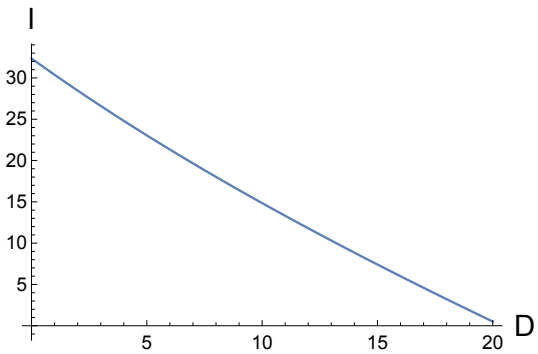

Fig. 3 Interpenetration length in terms of wall distance.

which is is expected. In Ref.[15], it is mentioned that interpenetration length in polymer brush bilayers at melt concentration scales as $\sim D^{-1/3}$ and at semidilute concentration as $\sim D^{-0.17}$. The wall distance appears to not to fulfill similarity rules. The reason might be due to the fact that the wall distance is not a molecular parameter.

In Fig. 4, I present Interpenetration length in terms of index of polymerization. I plot Eq. 23 and a power law fit as $\sim N^{0.976}$. This power law almost fits to Eq. 23. In Ref.[15], universal power law $\sim N^{2/3}$ and $\sim N^{0.51}$ respectively for melt and semidilute regimes are proposed. Naturally, as index of polymerization increases, longer polymer chains tend to increase interpenetration length.

In Fig. 5, I present interpenetration length in terms of second

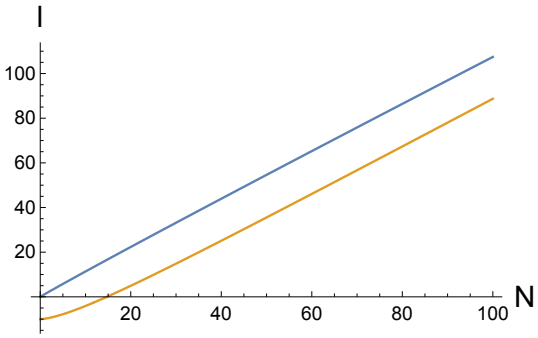

Fig. 4 Interpenetration length in terms of index of polymerization. Eq. 23 (orange) and universal scaling law $^{0.976}$ (blue).

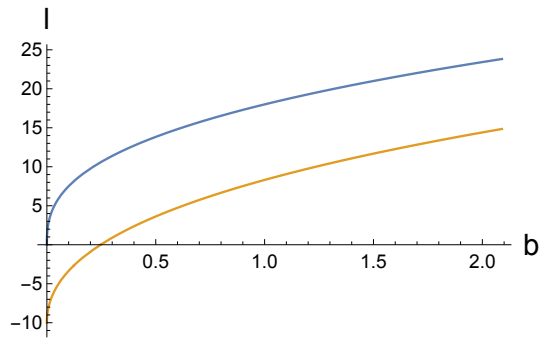

Fig. 5 Interpenetration length in terms of second virial coefficient. Eq. 23 (orange) and universal scaling law $\sim b^{0.38}$ (blue).

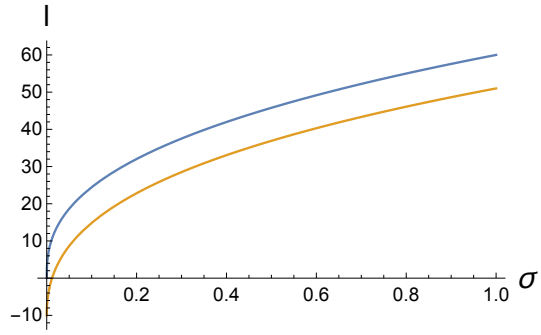

Fig. 6 Interpenetration length in terms of grafting density. Eq. 23 (orange) and universal scaling law $\sim \sigma^{0.39}$ (blue).

virial coefficient. Eq. 23 fits to power law $\sim b^{0.38}$. It is natural that brush bilayers respond to binary correlations among monomers. For instance, quality of solvent is determined by second virial coefficient as poor, theta or good solvent. In poor solvent conditions, the second virial coefficient is negative and monomers attract each other. Poor solvent conditions develop hydrophobic behavior of monomers[16]. As the second virial coefficient vanishes in a certain temperature, a theta solvent appears in which monomers do not go through binary correlations however there exists ternary correlations among them[16]. As the second virial coefficient gets positive values good solvent conditions appear where monomers take hydrophilic properties[16].

In Fig. 6, I show interpenetration length in terms of grafting density. This plot fits to power law $\sim \sigma^{0.39}$. In Ref.[15], interpenetration length is independent of grafting density for melts and it scales as $\sim \sigma^{-0.51}$ for semidilutes. However, one would criticize the results of Ref.[15] since the interpenetration length naturally must increase as number of chain per surface area increases.

In Fig. 7, I present interpenetration length in terms of segment length. This plot fits to power law $\sim a^{0.69}$. While Ref.[15] proposes a power law $\sim a^{4/3}$ for melts and $\sim a^{0.15}$ for semidilutes. The prediction of Ref.[15] about interpenetration at melts is quit close to my calculations.

The total grand free energy can be calculated by inserting Eq. (22) into grand free energy and after integration we obtain,

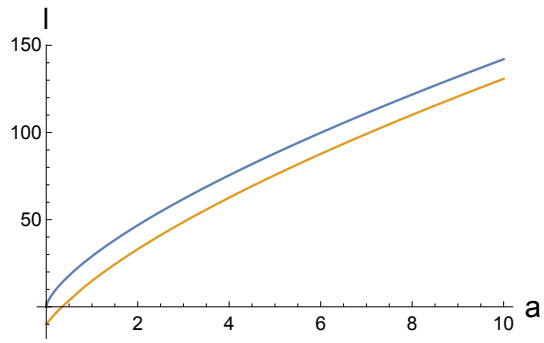

Fig. 7 Interpenetration length in terms of segment length. Eq. 23 (orange) and universal scaling law $\sim a^{0.69}$ (blue).

$$\begin{aligned}\Phi = & - \frac{k_B T}{120 a^4 b D^3 N^4}(435D^8 + 360a^2 b N^3 \sigma - 187D^7 \eta \\ & - 48a^2 b D N^3 \sigma \eta_1 \eta + 187D^6 \eta^2 - 150a^2 b N^3 \sigma \eta_1 \eta^2 \\ & + D^4 \eta_2 \eta + 2D^3 \eta_3 \eta^2) \end{aligned} \tag{24}$$

where I introduce volumes as,

$$\begin{aligned}\eta_1 &= \left(\sqrt{3a^2 b N^3 \sigma \left(3a^2 b N^3 \sigma - 2D^3\right)} + a^2 b N^3 \sigma\right) \\ \eta_2 &= \left(151\sqrt{3a^2 b N^3 \sigma \left(3a^2 b N^3 \sigma - 2D^3\right)} - 351a^2 b N^3 \sigma\right) \\ \eta_3 &= \left(169\sqrt{3a^2 b N^3 \sigma \left(3a^2 b N^3 \sigma - 2D^3\right)} - 558a^2 b N^3 \sigma\right)\end{aligned}$$

In Fig. (8), I present plots of Eq. (24) in terms of segment length and the second Virial coefficient. Both quantities influence the grand potential energy in a way extremely similar to each other. At small segment lengths and Virial coefficients, the grand potential energy approaches $-\infty$. At the middle values, the grand potential energy possesses an unstable maximum positive value and at large values the grand potential energy again decreases to negative values and approaches a certain negative value. Existence of an unstable maximum point in the grand potential energy indicates that there is a certain segment length and Virial coefficient in which the total energy of the system maximizes. However, the system is very unstable in this point and with the smallest fluctuation drops down. Moreover, there are two zero energy points in the plots.

In Fig. (9), I present plots of Eq. (24) in terms of wall distance and the index of polymerization. The grand potential in all wall distances is negative with a smooth minimum point in the middle. Existence of this stable minimum point indicates that the substrates tends to stay in this distance. Practically, it means that there is a certain wall distance below which the substrates repel each other and above which they attract each other. However, response of the grand potential under variation of the index of polymerization is very similar to segment length and the Virial coefficient regarding existence of an unstable maximum point.

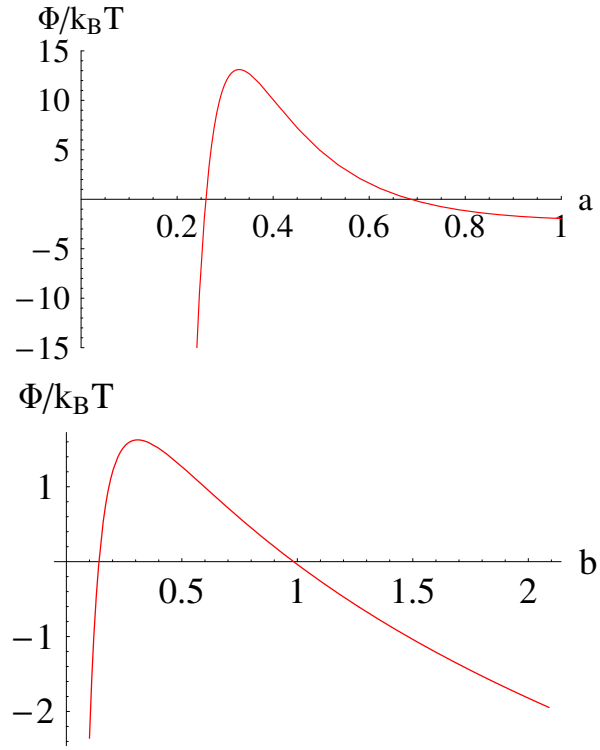

Fig. 8 Total grand potential in terms of segment length (left) and the second Virial coefficient (right).

Similarly, in a certain index of polymerization, the system reaches its maximum possible energy but small fluctuations make system away from this maximum energy. With long chains, the energy of the system changes its sign and approaches an asymptotic value. In general, it appears the molecular parameters corresponding to chains i.e. segment length, the second Virial coefficient and the index of polymerization influence the total energy in the same way.

In Fig. (10), I show the grand potential energy in terms of grafting density. The plot clearly indicates a universal power law in terms of grafting density. My fitting shows that the grand potential energy scales as $\sim \sigma^{1.5}$. It is showing that negativity of the grand potential energy increases by grafting density. Practically, it means that the substrates are attracted by each other as grafting density increases.

The energy due to binary correlations among monomers within the interpenetration region is obtained through inserting Eq. (22) into the third integral in Eq. (20) which gives us,

$$\begin{aligned}\Phi^l = & - \frac{k_B T}{15 a^4 b D^3 N^4}(42D^8 + 180a^2 b D^5 N^3 \sigma - 11D^7 \eta + 6a^2 b D N^3 \sigma \eta_1 \eta \\ & + 11D^6 \eta^2 + 30a^2 b N^3 \sigma \eta_1 \eta^2 + 2D^3 \eta_4 \eta^2 + D^4 \eta_5 \eta) \end{aligned} \tag{25}$$

where I introduce volumes as,

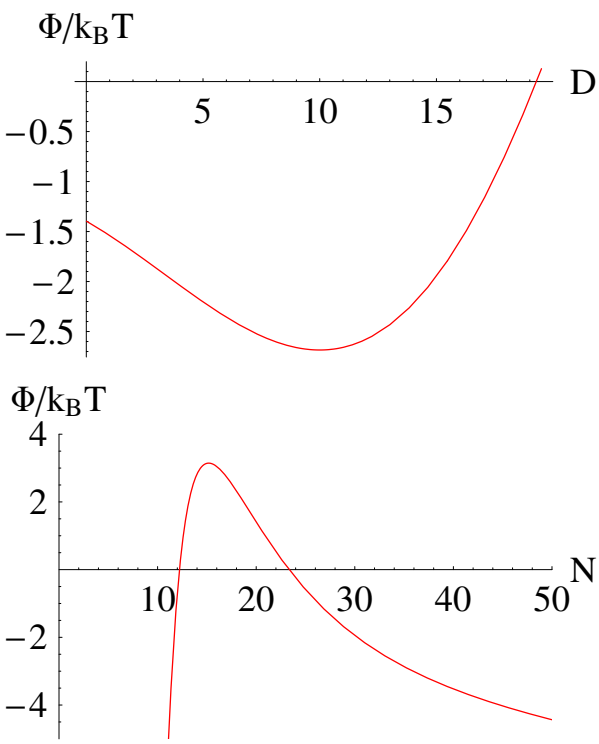

Fig. 9 Total grand potential in terms of wall distance (left) and the index of polymerization (right).

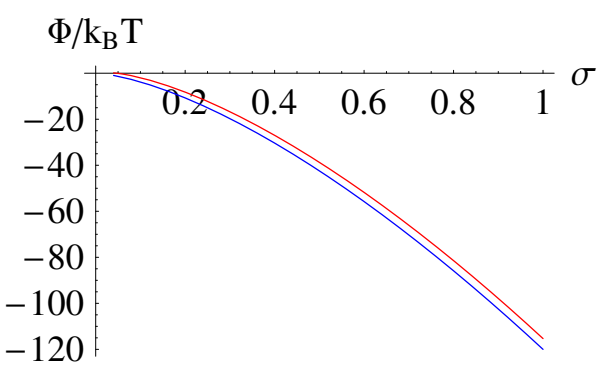

Fig. 10 Total grand potential in terms of grafting density Eq. (24) (red), power law $\sim \sigma^{1.5}$ fit (blue).

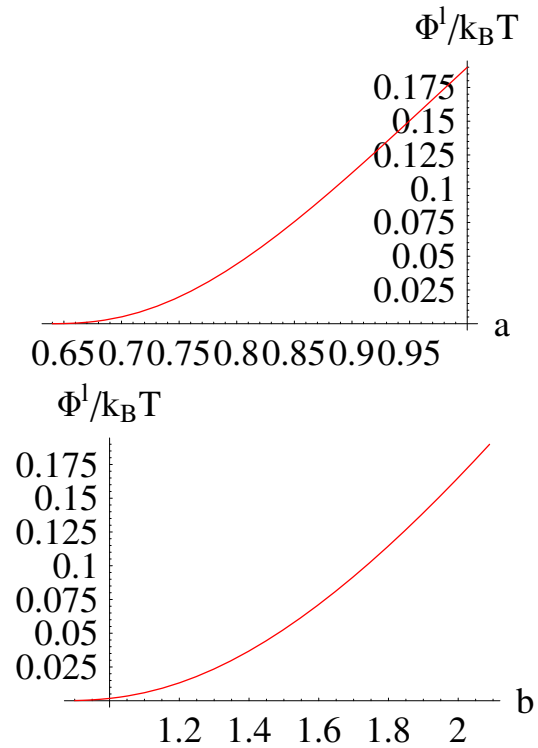

Fig. 11 Energy within the interpenetration length in terms of segment length (left) and the second Virial coefficient (right).

$$\eta_4 = \left(17\sqrt{3a^2bN^3\sigma\left(3a^2bN^3\sigma - 2D^3\right)} - 39a^2bN^3\sigma\right)$$

$$\eta_5 = \left(23\sqrt{3a^2bN^3\sigma\left(3a^2bN^3\sigma - 2D^3\right)} - 93a^2bN^3\sigma\right)$$

In Fig. (11), I present plots of Eq. (25) in terms of segment length and the second Virial coefficient. The plots indicate both parameters increase the energy within the interpenetration length.

In Fig. (12), I present plots of Eq. (25) in terms of the wall distance and the index of polymerization. In the case of variation of the index of polymerization, we observe a quit similar behavior with the segment length and the second Virial coefficient i.e. a non power law increment in energy. Nevertheless, the variation of wall distance influences the free energy within the interpenetration length as an increment at small distances, then an smooth maximum energy and subsequently, a reduction up to zero at large wall distances. Occurrence of a maximum point in a certain wall distance suggests that there is a threshold for the binary interactions among monomers within the interpenetration region. The threshold value occurs in large compression corresponding to small wall distances. The interesting outcome here is that the plot suggests that compressing more leads to less binary correlations among monomers withing the interpenetration region.

In Fig. (12), I present plots of Eq. (25) in terms of grafting density. Certainly, the plot indicates a power law. My fitting

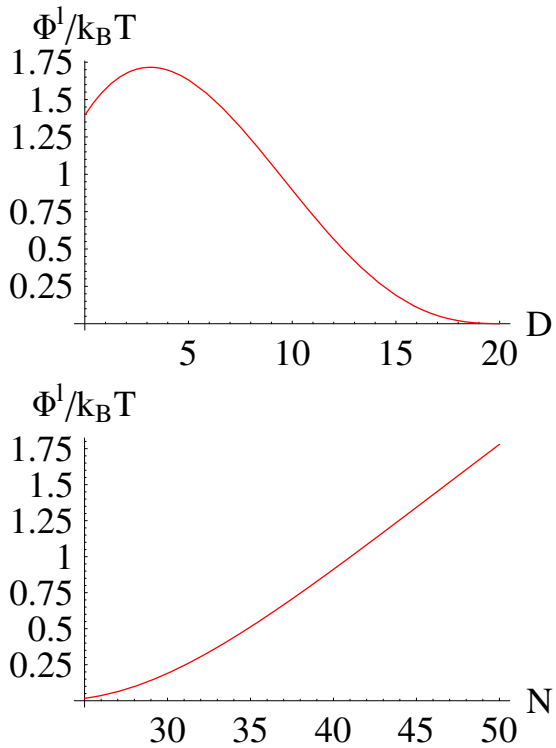

Fig. 12 Energy within the interpenetration length in terms of the wall distance (left) and the index of polymerization (right).

shows that the energy within the interpenetration length scales as $\sim \sigma^{1.8}$.

Taking derivative of Eq. (24) with respect to the wall distance produces the normal stress or pressure exerted on the bottom substrate at $z = 0$. Since, the system is at thermal equilibrium state, the pressure is the same throughout the medium. The derivative of grand potential energy gives the following pressure in terms of molecular parameters and wall distance,

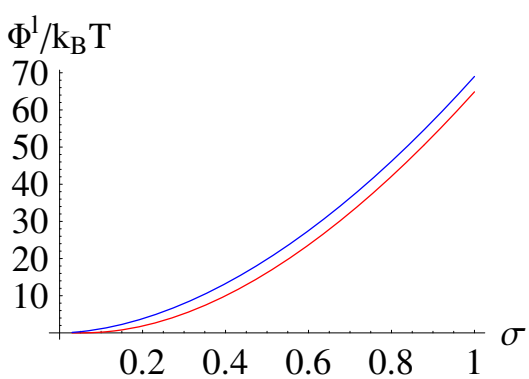

Fig. 13 Energy within the interpenetration length in terms of grafting density Eq. (25) (red), power law $\sim \sigma^{1.8}$ fit (blue).

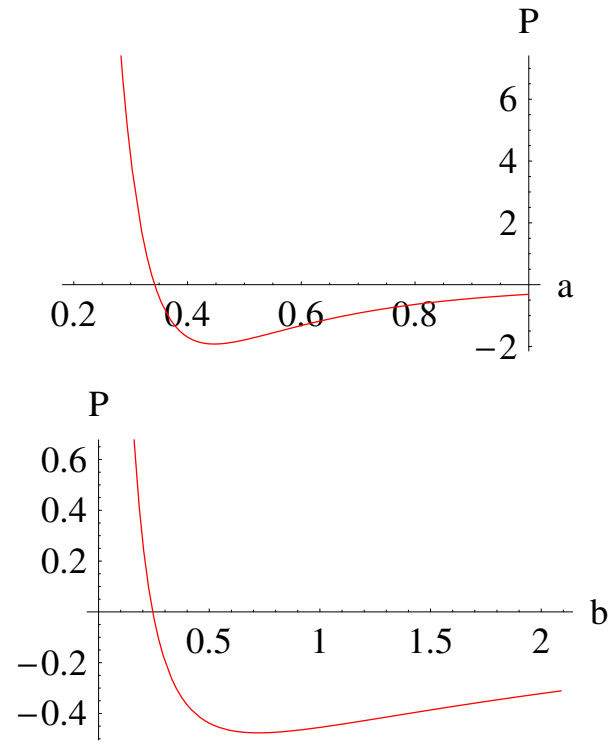

Fig. 14 The normal stress or pressure exerted on the bottom substrate in terms of the segment length (left) and the second Virial coefficient (right).

$$
\begin{aligned}
P &= \frac{k_B T}{24 a^4 b N^4 \chi \eta^2}(90\sqrt{3}a^6 b^3 N^9 \sigma^3 + D^4 \chi (187 D^2 - 187 D\eta + 435\eta^2) \\
&+ a^2 b D N^3 \sigma (548\sqrt{3}D^5 - 852 D^2 \chi + 174\sqrt{3}D^4 \eta - 231 D\chi\eta + 144\chi\eta^2) \\
&+ 9 a^4 b^2 N^6 \sigma^2 (10\chi - \sqrt{3}D^2(98D + 29\eta))) \qquad (26)
\end{aligned}
$$

where I introduce a volume χ as follows,

$$\chi = \sqrt{a^2 b N^3 \sigma(-2D^3 + 3a^2 b N^3 \sigma)}$$

In Fig. (14), I present plots of Eq. (26) in terms of the segment length and the second Virial coefficient. In principle, both quantities influence similarly the pressure. At small values, there is a infinitely large pressure in the z direction which decreases by the segment length and the second Virial coefficient. From then on, the pressure changes sign and orients in the negative z direction. After reaching an smooth maximum value in the negative z direction, the pressure again decreases and approaches a certain value.

In Fig. (14), I present plots of Eq. (26) in terms of the wall distance and the index of polymerization. It shows that the pressure is upward at high compression nevertheless it is downward at low compression. However, at high compression there is a very smooth maximum pressure. It is also showing that the pressure changes its orientation in the moderate compression. The index of polymerization influences pressure in a way that with short chains, pressure is downward and infinitely large while with long

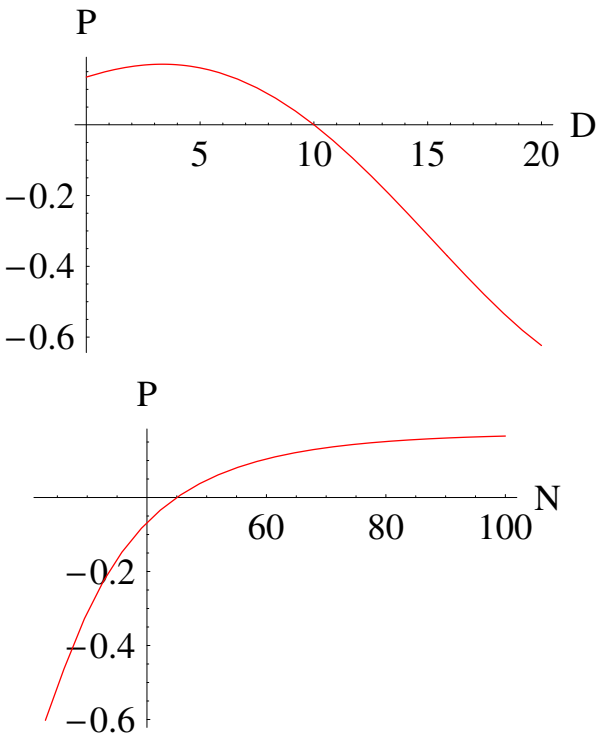

Fig. 15 The normal stress or pressure exerted on the bottom substrate in terms of the wall distance (left) and the index of polymerization (right).

chains, pressure becomes upward and reaches a certain asymptotic value.

In Fig. (16), I present plots of Eq. (26) in terms of grafting density. At low grafting densities, pressure is downward and small, however, it changes sign in moderate grafting densities and becomes upward for large grafting densities.

7 Conclusion and discussion

In this study, theoretically, I review the equilibrium properties of polymer chains with aiming at theoretical approach to polymer brush bilayers. I show how polymer brush covered surfaces interpenetrate in each other through giving approximate density profiles of two brushes. I also show how interpenetration length in polymer brush bilayers depend upon molecular parameters. The interpenetration length decreases by wall distance through a non-power law behavior. This suggests that the interpenetration length does not obey similarity rules. Although, it depends upon molecular parameters through universal power laws. All molecular parameters follow similarity rules among them index of polymerization (which scales linearly) influence the interpenetration length strongly, however, grafting density and the second Virial coefficient have influence it weakly. Calculations indicate that all molecular parameters increase interpenetration length though through different universal power law. This is an interesting outcome, for instance, in the case of the second Virial coefficient which describes strength of the binary correlations among monomers. I have considered the strength of the binary correlations among all monomers the same. One might say that increase in the interpenetration length due to binary correlations occurs because of repulsion among monomers inside brushes and not because of repulsion among monomers of different brushes within the interpenetration length. If one takes different binary correlations among monomers of top and bottom brushes, it will be shown that binary correlations among different brushes within the interpenetration length give rise to reduction of it.

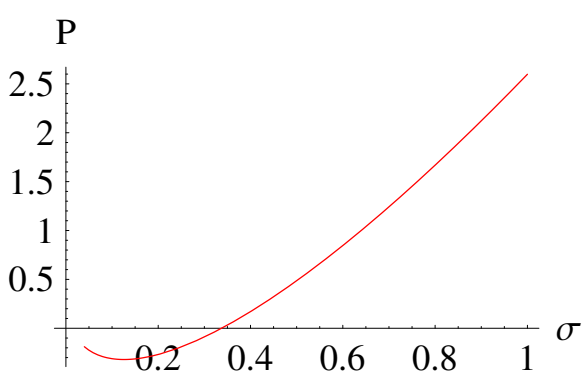

Fig. 16 The normal stress or pressure exerted on the bottom substrate in terms of grafting density.

The total energy, the energy within the interpenetration region and the normal stress throughout the system indicate existence of zero energy and zero pressure points upon wide range of possible values for parameters of the system. This can be an application oriented outcome of this research, since, one might become able to tune pressure orientation through playing with the segment length, strength of the binary correlations (different solvent qualities) and chain length. The most interesting outcome, in this context, would be ability to change the pressure orientation via tuning distance between substrates. It would be fascinating in lubrication technology if someone become able to tune the friction coefficient by choosing right distance between surfaces. For instance, my study suggests that strongly compressed brushes attract each other nevertheless weakly compressed brushes repel each other. So, one might only use weakly compressed brush covered surfaces for lubrication purposed. Another suggestion of this research would be to use short chains and lower grafting density to achieve repulsion of substrates. The reason for this claim is hidden in the complex interactions among monomers.

The significance of this study becomes more clear as it is a unique approach (to the best of my knowledge) to the problem of interpenetration of two soft materials by taking their simultaneous deformations into account. The simultaneous deformations is a key element in soft matter and biological systems.

The blob picture which have been utilized in Ref.[15] is seems to be extremely simple and it does not capture important details. For instance, as I showed, the interpenetration length is dependent upon binary correlations among monomers as well as it increases by grafting density, two facts that the blob picture method lacks. It is worth noting that since in biological macromolecules there are competitions among different interactions (such as elasticity, excluded volume etc), therefore approaches like blob picture are not able, intrinsically, to deliver sufficient information.

There are no conflicts to declare.

References

1 M. Rubinstein and R. Colby, *Polymer Physics*, OUP Oxford, 2003.

2 F. Schwabl and W. Brewer, *Statistical Mechanics*, Springer Berlin Heidelberg, 2006, pp. 313–316.

3 R. Advincula, W. Brittain, K. Caster and J. Rühe, *Polymer Brushes*, Wiley-VCH, Weinheim, 2004.

4 E. Zhulina and O. Borisov, *Journal of Colloid and Interface Science*, 1991, **144**, 507–520.

5 S. T. MILNER, *Science*, 1991, **251**, 905–914.

6 A. Halperin, M. Tirrell and T. P. Lodge, in *Tethered chains in polymer microstructures*, Springer Berlin Heidelberg, Berlin, Heidelberg, 1992, pp. 31–71.

7 S. T. Milner, T. A. Witten and M. E. Cates, *EPL (Europhysics Letters)*, 1988, **5**, 413.

8 I. Szleifer and M. A. Carignano, in *Tethered Polymer Layers*, Wiley-Blackwell, 2007, pp. 165–260.

9 J. Klein, D. Perahia and S. Warburg, *Nature*, 1991, **352**, 143.

10 H. J. Taunton, C. Toprakcioglu, L. J. Fetters and J. Klein, *Nature*, 1988, **332**, 712.

11 J. Klein, E. Kumacheva, D. Mahalu, D. Perahia and L. J. Fetters, *Nature*, 1994, **370**, 634.

12 T. Kreer, M. H. Müser, K. Binder and J. Klein, *Langmuir*, 2001, **17**, 7804–7813.

13 T. Kreer, K. Binder and M. H. MÃijser, *Langmuir*, 2003, **19**, 7551–7559.

14 A. Galuschko, L. Spirin, T. Kreer, A. Johner, C. Pastorino, J. Wittmer and J. Baschnagel, *Langmuir*, 2010, **26**, 6418–6429.

15 T. Kreer, *Soft Matter*, 2016, **12**, 3479.

16 P. G. Gennes, *Scaling Concepts in Polymer Physics*, Cornell University Press, 1979, pp. 74–75.